Indian Journal of Science and Technology, *Vol 12(9), DOI: 10.17485/ijst/2019/v12i9/140977, March 2019*
ISSN (Print) : 0974-6846
ISSN (Online) : 0974-5645

Synthesis and Characterization of Titanium Dioxide Nanoparticles with a Dosimetry Study of their Ability to Enhance Radiation Therapy using a Low Energy X-ray Source

Asma M. Alturki[1*] and Rachid Ayad[2]

[1]Department of Chemistry, Faculty of Science, University of Tabuk, Saudi Arabia; aallturky@ut.edu.sa
[2]Department of Physics, Faculty of Science, University of Tabuk, Saudi Arabia; rayad@ut.edu.sa

Abstract

Objective: This study was undertaken to synthesize and characterize TiO_2 NPs and to study the interaction of TiO_2 NPs with radiation and then estimate the Dose-enhancement Factor (DEF) at different concentrations of NPs under low-energy excitation (14-35 kV). **Methods**: Titanium dioxide (TiO_2) Nanoparticles (NPs) were synthesized by the sol-gel method. The structure, particle size and crystal phase were evaluated by Scanning Electron Microscopy (SEM), Transmission Electron Microscopy (TEM) and X-ray Diffraction (XRD). **Findings:** The XRD pattern exhibited peaks that were assigned to analyse crystals with particle sizes from 2-10 nm. The X-ray absorption of TiO_2 NP solutions and pure water were investigated. Solutions with 0, 3.33, 6.66 and 20% of the TiO_2 NPs were used to study the X-ray absorption of the samples and the Dose Enhancement Factor (DEF) is evaluated. The experimental results showed that the X-ray absorption for solutions with 0, 3.33, 6.66 and 20% of the TiO_2 NPs increased with increasing concentration for generated beams from 14 kV to 35 kV. Additionally, a Dose-enhancement Factor (DEF) was observed for low-energy beams between 14 kV and 35 kV. TiO_2 NPs at very low energies (14-35 kV) able to display significantly enhanced X-ray absorption, resulting in a higher absorbed dose. **Application/Improvements:** Many scientists have focused on nanoparticles, such as TiO_2 NPs, due to their numerous functions that enhance the nature of their antibacterial properties. Cancer is one of the reasons for human mortality. The main concept of cancer radiotherapy is the enhance radiation dose absorption at the targeted site by using high-Z materials.

Keywords: Dosimetry, Low Energy Source, Nanoparticles, Radiation Therapy, Titanium Dioxide

1. Introduction

Nanomaterials play a relevant role in different biomedical studies. NPs of metal oxide have attracted attention due to their unique properties. NPs can be synthesized by different methods, such as growth in solution, sol-gel, vapour deposition, pyrolysis and green biosynthesis methods[1]. Gold (Au) NPs (GNPs) as well as ZnO and TiO_2 NPs have been widely used in cancer treatment and phototherapy because of their low cost, nontoxicity and stability[2]. Many scientists have focused on the characterization of nanoparticles, such as TiO_2 NPs, due to their numerous functions that enhance the nature of their antibacterial properties[3]. Cancer is one of the reasons for human mortality. The main concept of cancer radiotherapy is the enhancement of the radiation dose by using high-Z materials[4]. Therefore, we can deliver the maximum dose possible to cancer cells and still protect normal cells. Radiosensitization depends on the concentration and size of NPs as well as the photon energy[5]. A previous study testing the concept of high-Z materials in mice showed remarkable tumour abatement without toxicity for mice that were irradiated after the injection of GNPs compared with that for mice irradiated without GNPs[6]. The

*Author for correspondence

DEF (Dose-enhancement Factor) was evaluated according to the following definition: The ratio of the average doses deposited in the tumour volume with and without nanoparticles after final irradiation[7]. Estimated the effects of GNPs on dose enhancement through radiation treatment at 140 kV and 6 MV. The results showed that for Ir-192 at 140 keV, in the presence of GNPs, the dose enhancement for a tumour with 7 mg Au/g was at least a factor of 2 and ranged from 1-7% at 4-6 MV, depending on the GNP concentration[8]. The DNA-nano interaction is one of the most interesting investigative areas for cancer therapy because of its combined gamma radiation and nanomaterial effects[9].

The aim of this work is to synthesize and characterize TiO_2 NPs, study the interaction of TiO_2 NPs with radiation and then estimate the Dose-enhancement Factor (DEF) at different concentrations of NPs under low-energy excitation (14-35 kV).

2. Materials and Methods

TTIP, Titanium Tetraisopropoxide (97% from Sigma Aldrich); acetic acid and hydrochloric acid (Sigma Aldrich); and isopropyl alcohol (RANKEM) were used.

2.1 Synthesis of TiO_2 Nanoparticles

TiO_2 NPs were prepared by the sol-gel method using Titanium Isopropoxide (TTIP, 97%, Sigma Aldrich) as a precursor as well as deionized water and isopropyl alcohol (RANKEM). A total of 40 ml of isopropyl alcohol was added to 10 ml of TTIP in a 200 ml beaker to form the first mixture. The first mixture solution was stirred for 30 minutes. For the hydrolysis reaction, we prepared a mixture of hydrochloric acid, 10 ml of deionized water and 10 ml of isopropyl alcohol and then added it dropwise to the first mixture. Then, the final mixture solution was stirred continuously for 4 hours, after which the mixture had converted to a gel. The mixture was centrifuged at 4000 rpm, washed and dried. The dried TiO_2 NPs were calcined at 300°C.

2.2 X-ray Diffraction (XRD)

The X-ray Diffraction (XRD) measurements were performed on TiO_2 nanoparticle powders using a diffractometer (Bruker Axs D8 Advance, Germany). CuKα radiation (λ= 1.54˚A) was used at a voltage of 40 kV and a current of 25 mA.

2.3 Scanning Electron Microscopy (SEM)

The surface topography of the pure TiO_2 nanoparticle powder was characterized using Scanning Electron Microscopy (JXA840 JEOL, SEM, Japan) at an accelerating voltage of 15 kV and a working distance of 10 m. The specimens were sputter-coated with carbon for energy dispersive X-ray (EDX) analysis.

2.4 Transmission Electron Microscopy (TEM)

The morphology and size of the TiO_2 nanoparticles were characterized using Transmission Electron Microscopy (TEM) using a JEOL 2100F TEM instrument operating at an accelerating voltage of 100 kV.

2.5 Evaluation of the X-ray Absorption of TiO_2 Nanoparticle Solutions

The X-ray measurements were performed using tube voltages between 14 kV and 35 kV at 1 mA. The X-ray beam was generated with a Molybdenum (Mo) anode X-ray tube: K_α = 17.4 keV (71.1 pm), K_β = 19.6 keV (63.1 pm). The High Voltage (HV) tube was scanned between 14 kV to 35 kV the HV range available in our X-ray source.

3. Results and Discussion

3.1 Characterizations

3.1.1 X-ray Diffraction (XRD)

The structure and particles size of the TiO_2 nanoparticle powder was determined by X-ray Diffraction. Figure 1 shows the XRD pattern of the TiO_2 NPs powder. Anatase peaks were observed at a 2θ of 52.47˚, 55.05˚, 63.44˚, 74.50˚ and 76.50˚; therefore, the major phase of our sample matched with the crystal faces of the anatase TiO_2 phase (105), (211), (204), (215) and (301), respectively, crystal planes, card 21-1272, JCPDS]. Rutile peaks are found at 2θ values of 14.42°, 29.62°, 44.48° and 66.75°; these correspond to crystal planes of (001), (110), (210) and (221) (JCPDS Card no. 21-1276). The anatase phase is preserved under 150°C, while the rutile phase is predominant at temperature higher than 250° C[10]. We evaluated the crystallite size from the X-ray diffraction results using the Scherrer equation: $D = K\lambda / \beta \cos\theta$, where λ is the wave-

length of the X-ray radiation, D is the crystallite size, K is a constant, β is the full width at half maximum (FWHM) (Cu Kα-1 radiation = 1.54060 Å), and θ is the Bragg angle of the peak[11]. From the XRD spectrum, the particle sizes ranged from 2-10 nm.

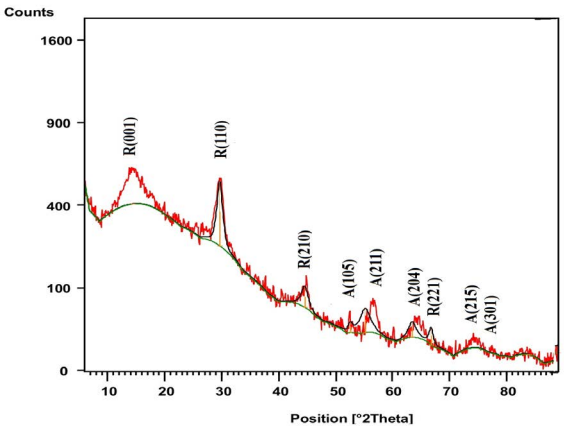

Figure 1. Pattern of the identified phases of TiO_2 NPs powder.

3.1.2 Scanning Electron Microscopy (SEM)

Figure 2 shows the SEM images of the prepared TiO_2 NPs. The surface morphology of the TiO_2 NPs was studied using scanning electron microscopy. The SEM images show that the NP conglomerate caused an increase in the TiO_2 NP size[12] and that the TiO_2 NPs had a uniform spherical morphology. Figure 3 shows the EDX spectrum of the TiO_2 NPs. The spectrum shows the chemical constituents present in the sample. The EDX spectrum shows that there is an impurity peak for carbon but that the majority of the sample is TiO_2, as shown in Table 1.

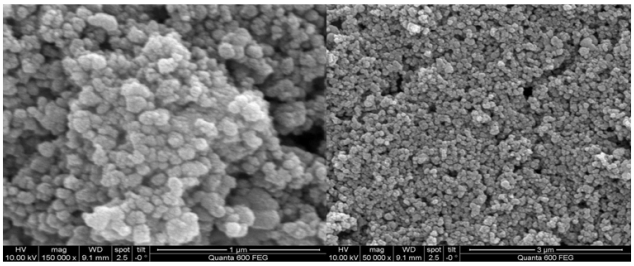

Figure 2. SEM images of prepared TiO_2 NPs.

3.1.3 Transmission Electron Microscopy (TEM)

The TEM image in Figure 4 shows the presence of nano-sized TiO_2 NPs, which can be ascribed to the anatase crystal phase. The uniform particles in the image of the TiO_2 NPs might be ascribed to the aggregation of small TiO_2 NPs during the growth of the nanocrystals. Therefore, the growth of these nanoparticles was uncontrolled, and the resulting particles were more aggregated, thus causing the larger particle size seen in the SEM images.

Table 1. The chemical composition of the TiO_2 NPs

Element	Wt%	At%
CK	07.91	18.88
OK	21.77	39.02
TiK	70.33	42.10
Matrix	Correction	ZAF

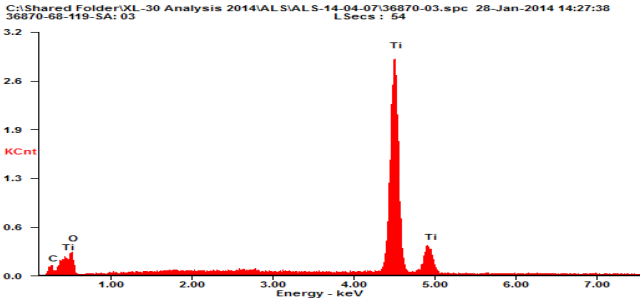

Figure 3. EDX of prepared TiO_2 NPs.

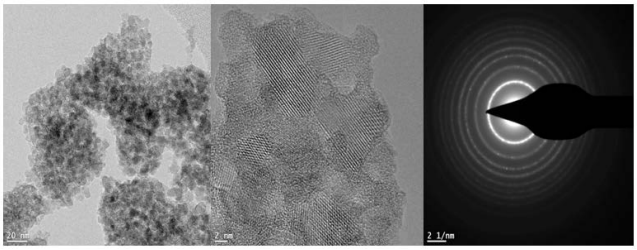

Figure 4. TEM images of the prepared TiO_2 TiO_2 NPs.

The microstructure of the TiO_2 NPs was obviously seen using TEM. In low-magnification images, spherical TiO_2 NPs with an average diameter of 10 nm were seen as shown in Figure 4(a), while Figure 4(b) shows the TiO_2 NPs at a higher magnification. The single-crystal TiO_2 NPs in Figure 4 were identifiable as the anatase phase (01-075-1537, JCPDS), with a spacing of 1.23 Å between the crystal planes.

3.2 TiO_2 (NPs) and Radiosynsitization

3.2.1 In vitro Studies of TiO_2 *NP Solutions*

X-ray beams were transmitted through pure water and TiO_2 NP solutions with different concentration of TiO_2

NPs (6.66, 13.23 and 20%). According to Figure 5, we can observe that the X-ray absorption for TiO_2 NP solutions is higher than the absorption of pure water. The amount of absorption increased with increasing TiO_2 NP percentage. At a voltage of 19 kV, which is near the k-edge of molybdenum, we see edge effect, for all weight percent samples. This is because X-ray attenuation increases at energies equal to the k-edge of the involved elements[13].

The effect of an increase in the *percentage* of TiO_2 NPs on the relative X-ray absorption at different X-ray tube voltages, from 14 to 35 kV, is shown in Figure 6. There exists an observable difference in the X-ray absorbance with and without TiO_2 NPs.

The maximum relative X-ray absorbance for samples with TiO_2 NPs was observed at 14 kV for a 20% by weight sample of TiO_2 NPs. In Figure 6, the results show that the absorbance of samples containing TiO_2 NPs under a 14 kV beam was higher than the absorbance under 24 and 34 kV for all samples with different weight percentages.

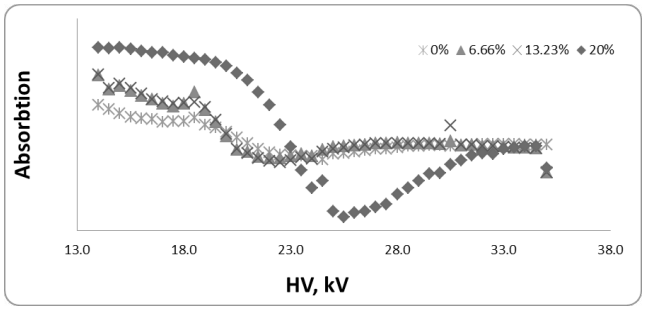

Figure 5. X-ray absorption for pure water and TiO_2 NPs solutions with different percentages of TiO_2 NPs.

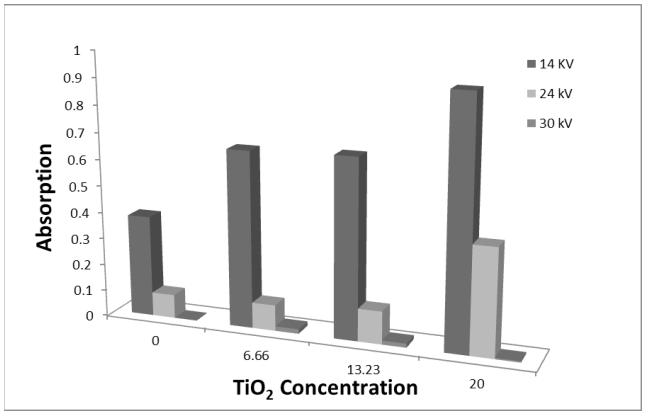

Figure 6. The effect of the TiO_2 NPs percentage on X-ray absorption at different HV.

3.2.2 Dose-enhancement Factor (DEF)

The effect of various NP concentrations on dose enhancement was measured at different HV for TiO_2 NPs in water and NPs solution at room temperature.

Figure 7 shows that the dose is always enhanced for any HV in the range of 14–35 keV but that the largest dose enhancements are achieved when HV was 35 keV.

This increase is due to lower absorption. The dose enhancement was higher with the addition of TiO_2 NPs due to the capability of promoting photoelectric interactions within NPs of heavy metals. The photoelectric effect occurred in the kV energy range, but lower kV energy radiation was capable of deeper permeation[14].

The best dose enhancements were obtained at the higher concentrations of TiO_2 NPs. The Dose-enhancement Factor (DEF) increased with increasing TiO_2 NP concentration as shown in Table 2.

Figure 7 shows the DEF as a function of the TiO_2 NP concentration for three different energy levels (14, 24 and 30 kV). The Dose-enhancement Factor increased almost linearly with increasing TiO_2 NP concentration. Figure 7 shows the Dose-enhancement Factor as a function of HV for all three different TiO_2 NP concentrations at 14 kVexcitation. The DEF is maximum at 14 kV for all concentrations.

DEF in the observed range of energy is facilitated by the increased interaction cross-section at the higher Z-number of titanium and the production of Auger electrons[15]. Some of these electrons may participate in dose enhancement.

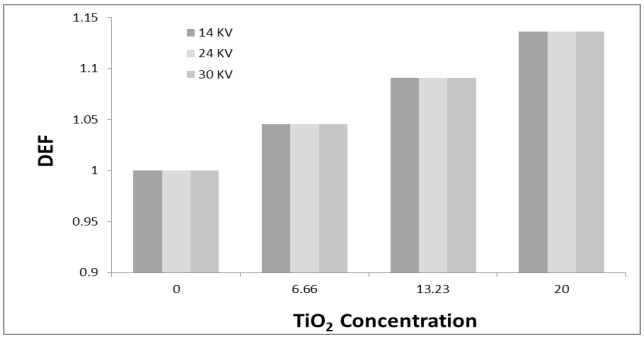

Figure 7. DEF as a function of the TiO_2 NPs concentration for three different HV values (14, 24 and 30 kV).

Table 2. Relation between TiO_2 NPs (%) and DEF

TiO_2 NPs (%)	DEF
0	1
6.66	1.045339
13.23	1.090678
20	1.136017

4. Conclusions

TiO_2 nanocomposites were prepared by mixing TiO_2 nanoparticles in a chitosan polymer. The XRD spectrum and TEM profile exhibited peaks that were assigned to the anatase crystal phase, with particle sizes of <10 nm. The maximum relative X-ray absorbance for the samples with TiO_2 NPs was observed at 14 kV for a 20% by weight sample of TiO_2 NPs. The optimum HV for the maximum dose enhancement of the TiO_2 NP solution was found to be approximately 14 kV for all concentrations.

5. Acknowledgements

The authors would like to acknowledge financial support for this work, from the Deanship of Scientific Research (DSR), University of Tabuk, Tabuk, Saudi Arabia, under grant no. S-1439-0079.

6. References

1. Babu EP, Subastri A, Suyavaran A, Rao PL, Kumar MS, Jeevaratnam K, Thirunavukkarasu C. Extracellularly synthesized ZnO nanoparticles interact with DNA and augment gamma radiation induced DNA damage through reactive oxygen species. RSC Advances. 2015; 5(76):62067–77. https://doi.org/10.1039/C5RA09935H
2. Nia MH, Tavirani MR, Nikoofar AR, Masoumi H, Nasr R, Hasanzadeh H, Jadidi M, Shadnush M. Stabilizing and dispersing methods of TiO_2 nanoparticles in biological studies. Journal of Paramedical Sciences. 2015; 6(2):69–105.
3. Kavitha K, Prabhu M, Rajendrana V, Manivasankan P, Prabu P, Jayakumar T. Optimization of nano-titania and titania–chitosan nanocomposite to enhance biocompatibility. Current Nanoscience. 2013; 9(3):308–17. https://doi.org/10.2174/1573413711309030003
4. Hainfeld J, Slatkin D, Smilowitz H. The use of gold nanoparticles to enhance radiotherapy in mice. Physics in Medicine and Biology. 2004; 49(18):309–24. https://doi.org/10.1088/0031-9155/49/18/N03
5. Anijdan SHM, Shirazi A, Mahdavi SR, Ezzati A, Mofid B, Khoei S, Zarrinfard M A. Megavoltage dose enhancement of gold nanoparticles for different geometric set-ups: Measurements and Monte Carlo simulation. International Journal of Radiation Research. 2012; 10(3-4):183–6.
6. Cho SH, Jones BL, Krishnan S. The dosimetric feasibility of Gold Nanoparticle-aided Radiation Therapy (GNRT) via brachytherapy using low-energy gamma-/X-ray sources. Physics in Medicine and Biology. 2009; 54(16):4889–905. PMid: 19636084 PMCid: PMC3064075. https://doi.org/10.1088/0031-9155/54/16/004
7. Su XY, Liu PD, Wu H, Gu N. Enhancement of radiosensitization by metal-based nanoparticles in cancer radiation therapy. Cancer Biology and Medicine. 2005; 11(2):86–91.
8. Cho SH. Estimation of tumor dose enhancement due to gold nanoparticles during typical radiation treatments: A preliminary Monte Carlo study. Physics in Medicine and Biology. 2005; 50(15):63–173. PMid: 16030374. https://doi.org/10.1088/0031-9155/50/15/N01
9. Liu Y, Zhang Y, Wang S, Pope C, Chen W. Optical behaviors of ZnO-porphyrin conjugates and their potential applications for cancer treatment. Applied Physics Letters. 2008; 92(14):143901. https://doi.org/10.1063/1.2908211
10. Li W, Liang R, Hu A, Huang Z, Zhou YN. Generation of oxygen vacancies in visible light activated one-dimensional iodine TiO_2 photocatalysts. RSC Advances. 2014; 4(70):36959–66. https://doi.org/10.1039/C4RA04768K
11. Zhao Y, Li C, Liu X, Gu F, Jiang H, Shao W, Zhang L, He Y. Synthesis and optical properties of TiO_2 nanoparticles. Materials Letters. 2007; 61(1):79–83. https://doi.org/10.1016/j.matlet.2006.04.010
12. Sugapriya S, Sriram R, Lakshmi S. Effect of annealing on TiO_2 nanoparticles. Optik. 2013; 124(21):4971–5. https://doi.org/10.1016/j.ijleo.2013.03.040
13. Panta RK, Bell ST, Healy JL, Aamir R, Bateman CJ, Moghiseh M, Butlera APH, Anderson NG. Element-specific spectral imaging of multiple contrast agents: A phantom study. Journal of Instrumentation. 2018; 13:1–18. https://doi.org/10.1088/1748-0221/13/02/T02001
14. Celina Y, Kyle B, Wonmo S, Jan S, Devika C. Determining the radiation enhancement effects of gold nanoparticles in cells in a combined treatment with cisplatin and radiation at therapeutic megavoltage energies. Cancers. 2018; 10(5):e150-e150. PMid: 29786642 PMCid: PMC5977123. https://doi.org/10.3390/cancers10050150
15. Georg H, Philipp M, Gotz P, Vladimir B, Wilhelm K, Hiltraud H, Jens F, Matthias K, Felix B, Frederik W, Michael H. Dose enhancement effects of gold nanoparticles specifically targeting RNA in breast cancer cells. PLOS ONE. 2018; 13(1):e0190183.